Title of the Project:

The Walk of Maximal Planar Graphs

By:

Lee Zheng Han

Institute:

NUS High School, Singapore

Mentor:

Mr Chia Vui Leong

The Walk of Maximal Planar Graphs

Abstract

Polyhedral combinatorics has been a topic of interest in modern day's computational geometry. The founding of Steinitz's Theorem in 1922 revealed consequential relations between graph theory and polyhedral combinatorics. It allows us to better investigate on the topology of convex polyhedrons. In this paper, we proposed an algorithm that generates a unique sequence of points, using the vertices of a triangulated polyhedron, pre-determined by the selection of the starting 3 vertices in the sequence. Following that, we discover an interesting relation between the sequence and the volume of the polyhedron itself, in which we presented in the form of a sufficient condition. To further investigate which polyhedrons generate sequences that satisfy the sufficient condition, we study the problem in the context of graph theory, that is, the explorer walk (corresponding to the sequence of vertices) in maximal planar graphs (skeletons of triangulated convex polyhedrons). With that, we uncovered a family of maximal planar graphs, called the explorer graphs, which exhibits volumetric properties in the polyhedrons constructed from them, in regard to the explorer walk. In this paper, we also introduce generalized methods of constructing explorer graphs of higher order from explorer graphs of lower order, demonstrating the prevalence of explorer graphs. As the edges of a maximal planar graph is of great importance in tracing an explorer walk, we investigate on the line graph of maximal planar graphs, and re-establish a better definition of explorer graphs. Lastly, our paper covers the edge contraction of explorer graphs, which allows us to solve the volume of polyhedrons constructed from non-explorer graphs. For this, we presented a possible bound for the minimum number of edge contractions a non-explorer graph requires from an explorer graph. This will generalize the proposed method of finding volumes to any triangulated convex polyhedron.

The Walk of Maximal Planar Graphs

Introduction

It is known in computational geometry that any n-gon (for $n \geq 4$) can be divided into $n - 2$ triangles, without gaps and overleaps, by the addition of $n - 3$ diagonals [1]. This process is commonly referred to as triangulation. Our research focuses solely on convex polyhedrons due to specific considerations that will be presented in the paper. Throughout our entire paper, a triangulated polyhedron refers to a convex polyhedron whose faces are triangulated. This is not to be confused with the triangulation of polyhedrons into tetrahedrons [6].

Explorer Order

Consider a convex polyhedron with n vertices. Any means of the triangulations can be applied to its faces such that every existing and new edge is shared by exactly two triangular faces. Now, suppose that we want to generate a sequence of points using the set of vertices from the polyhedron, and we desire such a sequence to be as unique as possible. The order of points in this sequence can be generated via the following algorithm (we call it the "**explorer order**"):

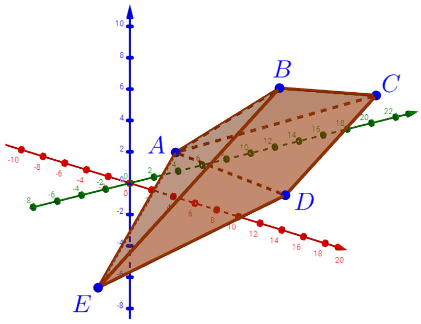

Figure 1

1. The starting three points corresponds to a triangular face in the anticlockwise manner
2. Any consecutive 3 points in the sequence corresponds to a triangular face
3. Any consecutive 4 points in the sequence are distinct
4. The sequence ends when
    a. The last 2 points in the sequence is the replica of the first two points in the same order and
    b. The 3rd point and the 3rd last point are distinct

It is easily observable that the order of points in the sequence is pre-determined by the selection of the first three points.

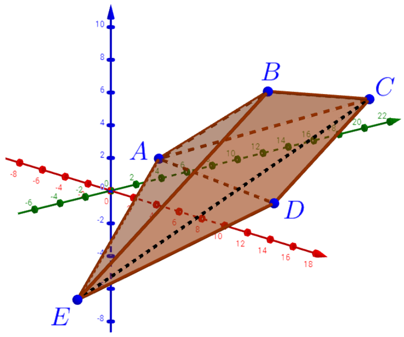

Figure 2

In Figure 2, we have triangulated *BCDE* from Figure 1 by adding the edge *CE*. Suppose we let "*ABC*" be the first three points. The following sequence can be obtained through explorer order:

"*ABCEDACBEADCEBACDEAB*"

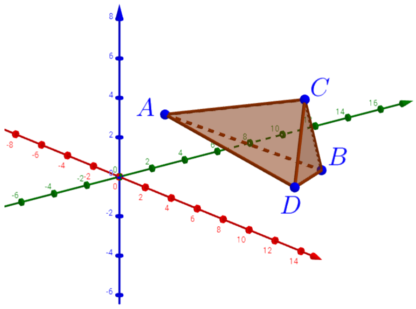

Figure 3

In Figure 3, we have a tetrahedron that contains only triangular faces. Suppose we let "*ABD*" be the first three points. The following sequence can be obtained through explorer order:

"*ABDCAB*"

The explorer order has undoubtedly provided a systematic way of tracing the vertices of a polyhedron, but at the same time, it appears to have properties for volume computation.

Alternating Shoelace Multiplication

Here, we introduce a set of notations for the **polarity** of the cross multiplication in a matrix. For any 3 points (may not be distinct) P_1, P_2 and P_3:

$$|P_1P_2P_3|^+ = \begin{vmatrix} x_1 & x_2 & x_3 \\ y_1 & y_2 & y_3 \\ z_1 & z_2 & z_3 \end{vmatrix} = \left(x_1y_2z_3 \quad x_3y_2z_1\right) \text{ and } |P_1P_2P_3|^- = \begin{vmatrix} x_1 & x_2 & x_3 \\ y_1 & y_2 & y_3 \\ z_1 & z_2 & z_3 \end{vmatrix} = \left(x_3y_2z_1 \quad x_1y_2z_3\right)$$

The above matrixes can be interpreted as products represented by diagonal arrows pointing downwards subtracting products represented by diagonal arrows pointing upwards.
For matrices containing $n \geq 4$ points ($P_1, P_2, P_3, \ldots, P_n$):

$$|P_1P_2P_3P_4P_5\ldots P_n| = \begin{cases} |P_1P_2P_3|^+ + |P_2P_3P_4|^- + |P_3P_4P_5|^+ + \ldots + |P_{n-2}P_{n-1}P_n|^- \\ = \sum_{r=1}^{(n-2)/2} \left(|P_{2r-1}P_{2r}P_{2r+1}|^+ + |P_{2r}P_{2r+1}P_{2r+2}|^- \right), & n = 2k+2,\ k \in \mathbb{Z}^+ \\ |P_1P_2P_3|^+ + |P_2P_3P_4|^- + |P_3P_4P_5|^+ + \ldots + |P_{n-2}P_{n-1}P_n|^+ \\ = |P_{n-2}P_{n-1}P_n|^+ + \sum_{r=1}^{(n-3)/2} \left(|P_{2r-1}P_{2r}P_{2r+1}|^+ + |P_{2r}P_{2r+1}P_{2r+2}|^- \right), & n = 2k+3,\ k \in \mathbb{Z}^+ \end{cases}$$

We define such multiplication method within a matrix to be the "**Alternating Shoelace Multiplication**". This method of multiplication is specially designed for matrices containing sequences of points generated through explorer order.

Suppose the pyramid shown in Figure 2 has vertices with coordinates *A(2, 2, 2)*, *B(6, 7, 6)*, *C(6, 15, 4)*, *D(11, 3, 1)* and *E(16, –17, 0)*. We have, by applying the alternating shoelace method on a matrix containing the sequence generated through explorer order in preceding section,

$$|ABCEDACBEADCEBACDEAB|$$

$$= \begin{vmatrix} x_1 & x_2 & x_3 & x_5 & x_4 & x_1 & x_3 & x_2 & x_5 & x_1 & x_4 & x_3 & x_5 & x_2 & x_1 & x_3 & x_4 & x_5 & x_1 & x_2 \\ y_1 & y_2 & y_3 & y_5 & y_4 & y_1 & y_3 & y_2 & y_5 & y_1 & y_4 & y_3 & y_5 & y_2 & y_1 & y_3 & y_4 & y_5 & y_1 & y_2 \\ z_1 & z_2 & z_3 & z_5 & z_4 & z_1 & z_3 & z_2 & z_5 & z_1 & z_4 & z_3 & z_5 & z_2 & z_1 & z_3 & z_4 & z_5 & z_1 & z_2 \end{vmatrix}$$

$$= \begin{vmatrix} 2 & 6 & 6 & 16 & 11 & 2 & 6 & 6 & 16 & 2 & 11 & 6 & 16 & 6 & 2 & 6 & 11 & 16 & 2 & 6 \\ 2 & 7 & 15 & -17 & 3 & 2 & 15 & 7 & -17 & 2 & 3 & 15 & -17 & 7 & 2 & 15 & 3 & -17 & 2 & 7 \\ 2 & 6 & 4 & 0 & 1 & 2 & 4 & 6 & 0 & 2 & 1 & 4 & 0 & 6 & 2 & 4 & 1 & 0 & 2 & 6 \end{vmatrix}$$

$$= 1206$$

The obtained value is discovered to have relations with the volume of the pyramid, which can be calculated through the summation of the determinants of all triangular faces of the triangulated pyramid in the anticlockwise manner [4].

$$Volume = \frac{1}{6}\left(\det|ABC| + \det|AEB| + \det|ADE| + \det|ACD| + \det|CBE| + \det|CED|\right)$$

$$= \frac{1}{6}\left(\begin{array}{l} \det\begin{vmatrix} 2 & 6 & 6 \\ 2 & 7 & 15 \\ 2 & 6 & 4 \end{vmatrix} + \det\begin{vmatrix} 2 & 16 & 6 \\ 2 & -17 & 7 \\ 2 & 0 & 6 \end{vmatrix} + \det\begin{vmatrix} 2 & 11 & 16 \\ 2 & \cancel{3} & 17 \\ 2 & 1 & 0 \end{vmatrix} \\ + \det\begin{vmatrix} 2 & 6 & 11 \\ 2 & 15 & 3 \\ 2 & 4 & 1 \end{vmatrix} + \det\begin{vmatrix} 6 & 6 & 16 \\ 15 & 7 & -17 \\ 4 & 6 & 0 \end{vmatrix} + \det\begin{vmatrix} 6 & 16 & 11 \\ 15 & 17 & \cancel{3} \\ 4 & 0 & 1 \end{vmatrix} \end{array} \right)$$

$$= 201\ units^3$$

It is observable that the volume of the pyramid is one sixth of 1026 itself.

$$Volume = \frac{1}{6}\left|ABCEDACBEADCEBACDEAB\right| = 201\ units^3$$

It is natural for one to question the generality of using the explorer order in the computation of a polyhedron's volume. In fact, it can be easily verified that this method doesn't work for any triangulated polyhedron in general. Using the tetrahedron *ABCD* illustrated in Figure 3 as an example, let the coordinates of the vertices be *A(1, 2, 3)*, *B(3, 10, –1)*, *C(8, 5, 5)*, and *D(11, 2, 2)*. Using the existing formula, the volume of the tetrahedron is:

$$\begin{aligned} Volume &= \frac{1}{6}\left(\det\left|ABD\right| + \det\left|ADC\right| + \det\left|ACB\right| + \det\left|BCD\right|\right) \\ &= 55\ units^3 \end{aligned}$$

However, the value calculated from inputting the sequence of points that we have generated earlier into the matrix is:

$$\begin{aligned} \frac{1}{6}\left|ABDCAB\right| &= \frac{1}{6}\begin{vmatrix} 1 & 3 & 11 & 8 & 1 & 3 \\ 2 & 10 & 2 & 5 & 2 & 10 \\ 3 & -1 & 2 & 5 & 3 & -1 \end{vmatrix} \\ &= -\frac{155}{6}\ units^3 \end{aligned}$$

Problem Statement

Our research aims to find which triangulated convex polyhedrons whose volume can be calculate via the means of explorer order.

Sufficient Condition

Like the case of tetrahedrons, the proposed explorer order doesn't solve for the volumes of many triangulated polyhedrons that we verified. For example, it doesn't solve the volume of polyhedrons with 4 or 6 vertices, no matter how they are triangulated. It is therefore challenging to find more cases in which the explorer order can be used to calculate volumes like the pyramid. We must have an indication, without verifying using other methods, that the value obtained via the means of explorer order on a certain triangulated polyhedron is the volume. We, hence, arrive at the following sufficient condition:

Result 1:

Using the vertices of any triangulated polyhedron with *F* triangular faces, we will be able to find a sequence of points via explorer order. 1/6 of the value obtained by applying the Alternating Shoelace Multiplication on a matrix containing the sequence is volume of the polyhedron if the sequence contains *3F + 2* points. (For proof, see "Appendix")

Our counter example of tetrahedron satisfies the contrapositive of the condition. It is true that the explorer order did not generate *3F + 2 = 14* points since the resulting value doesn't not match the volume of the tetrahedron. The Euler's Polyhedral Formula states that the number of faces *F* (in our case, we are considering triangular faces of the triangulated polyhedrons), vertices *V*, and edges *E* of a convex polyhedron must satisfy *V* + *F* – *E* = 2. [3] Hence, the condition can also be restated as "the explorer order calculates the volume of a triangulated polyhedron if it generates *3E – 3V + 8* points in the matrix."

Triangulated Polyhedrons to Maximal Planar Graphs

Steiniz's Theorem states that "every convex polyhedron forms a 3-connected planar graph, and every 3-connected planar graph can be represented as the graph of a convex polyhedron." [2] To solve the problem of tracing vertices via explorer order in a triangulated polyhedron, we ignore the specific coordinates of its vertices and translate it into a planar graph (containing f faces, e edges and v vertices) that should be a maximal planar graph.

There are existing methods of embedding convex polyhedrons into polyhedral graphs. We are only adding a restriction that all faces of the polyhedrons must already be triangulated. This can roughly be done by randomly selecting a triangular face and expanding it for the rest of the triangulated polyhedron to be flattened upon, resolving the problem into a graph theory question.

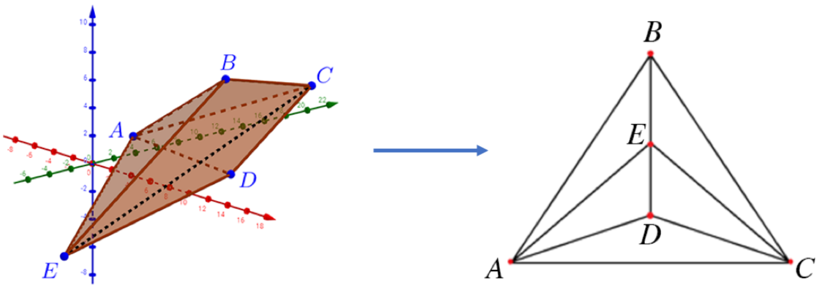

Figure 4

Figure 4 shows a triangulated pyramid, where $F = 6$ (note that AD is an edge, with triangles ADE and ADC as 2 faces), $E = 9$ and $V = 5$, and its corresponding maximal planar graph, where $f = 6$, $e = 9$ and $v = 5$.

The orientation of the bounded faces in the obtained maximal planar graph is equivalent to the original polyhedron's surface. ("ABC" is anti-clockwise on both the surface of the original polyhedron and its maximal planar graph) The outer triangle (instead of the unbounded region) in the graph also corresponds to a triangular face in the original polyhedron, but in the opposite orientation. Therefore, we may just treat the unbounded region as a face by convention.

> **Definition 1:**
>
> An explorer order of a triangulated polyhedron's vertices corresponds to a walk in its graph, we call it an "**explorer walk**".

Other polyhedrons that are not convex polyhedrons include toroidal polyhedrons. Such polyhedrons cannot be converted into maximal planar graphs. Hence, our research focuses solely on convex polyhedrons.

Explorer Graphs

Consider a polyhedron containing a way of triangulation that enables explorer order to calculate its volume. Its corresponding maximal planar graph can also be constructed into some other polyhedrons containing the same number of vertices but are topologically distinct. It is, hence, methodologically easier to work on explorer walks in maximal planar graphs than to apply explorer order on polyhedrons in a case-by-case basis. It is known that a maximal planar graph (containing v vertices) contains $3v - 6$ edges [7].

Definition 2: **Explorer Graphs** are maximal planar graphs (containing e edges and v vertices) that contains an explorer walk that generates $3e - 3v + 8 = 6v - 10$ points.

Revised Problem Statement 1: Our research aims to find explorer graphs. After which, we can then find all polyhedrons that can be constructed from these graphs.

A maximal planar graph is either an explorer or a non-explorer graph.

<u>Analysis of Explorer Graphs with n vertices ($4 \leq n \leq 6$)</u>
Now, we are in the position to analyze the existence of explorer graphs for small number of vertices ($4 \leq n \leq 6$).

For $n = 4$,
The complete graph on 4 vertices, K_4, is the unique maximal planar graph, and it is a non-explorer graph (K_4 is a tetrahedral graph). Hence, no explorer graph exists for $n = 4$.

For $n = 5$,
In [5], it is shown that there is a unique maximal planar graph with 5 vertices, which is shown in Figure 5. It is an explorer graph (corresponding to the skeleton of both triangulated pyramids and triangular bipyramids). Hence, no non-explorer graph exists for $n = 5$.

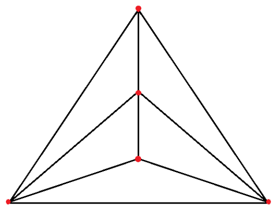

Figure 5

For $n = 6$,
In [5], it is shown that there exist only 2 non-isomorphic maximal planar graphs, and both graphs (Figure 6) are non-explorer. Hence, no explorer graph exists for $n = 6$.

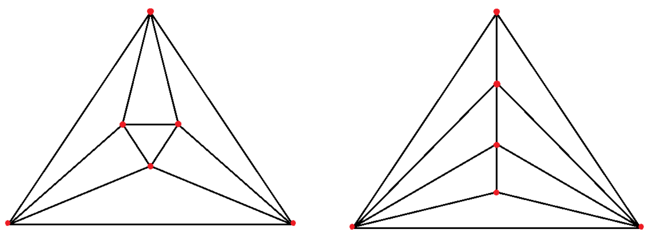

Figure 6

There exist both explorer and non-explorer graphs for $n > 6$ vertices. We hereby provide a way of constructing explorer graphs of a higher order from explorer graphs of a lower order.

<u>Construction of Explorer Graphs</u>
Following the definition of "edge contraction" used by Kenneth H. Rosen [8], an edge contraction of a simple graph will remain as a simple graph, implying that the creation of multiple edges and loops is not allowed.

Note that an edge contraction in a maximal planar graph is the loss of 1 vertex, 3 edges and 2 faces. In Figure 7, for example, edge AB is contracted. Following the contraction is the merging of edges Ap and Bp, Aq and Bq, and the loss of two triangular faces ABp and ABq.

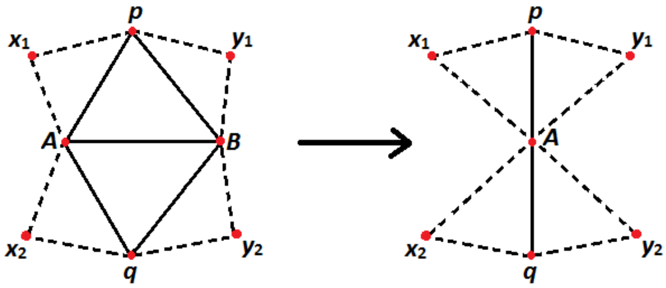

Figure 7

Hence, we define the "inverse" edge contraction on a *plane graph* to be the creation of 1 vertex, 3 edges and 2 faces. (Not to be confused with *vertex cleaving*) Referring to Figure 8, for example, we can choose vertex A and the two incident edges pA and qA to be involved in the operation. Ap and Aq divide the other vertices, which are adjacent to A, into 2 sides, say $X = \{x_1, x_2, x_3, \ldots, x_m\}$ and $Y = \{y_1, y_2, y_3, \ldots, y_n\}$, for some non-negative integers m and n.

The operation begins with the creation of a new vertex, B, and the edge AB. Accompanying that is the splitting of edges Ap into Ap and Bp, and Aq into Aq and Bq. In the case of Figure 8, $Y = \{y_1, y_2\}$ is reconnected to B, for the resulting graph to remain as a *plane graph*.

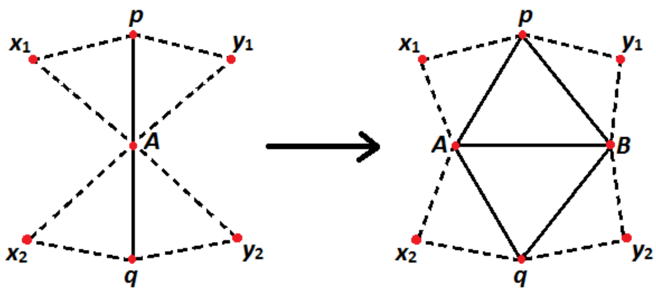

Figure 8

Result 2a:

For a plane graph of an explorer graph, P, applying the following string of "inverse" edge contractions on any vertex produces another explorer graph.

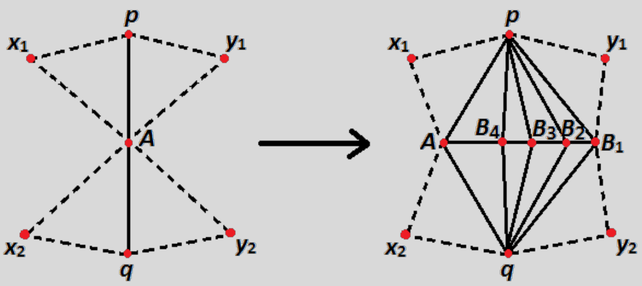

Result 2b:

For a plane graph of an explorer graph, P, applying the following string of "inverse" edge contractions on any vertex produces another explorer graph.

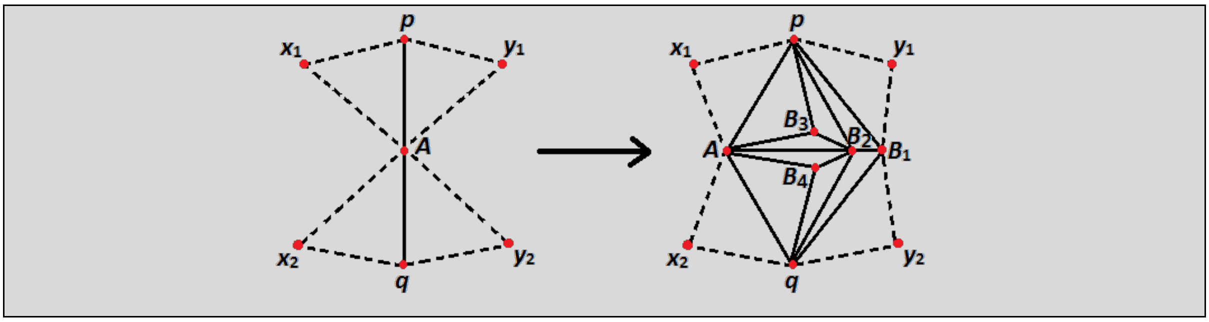

<u>1-directional classes</u>

In this section, 3 examples of "1-directional classes" of explorer graphs are constructed as a corollary of *Result 2a*. Now, the idea of *edge subdivision operation* shall be introduced as follows:

Let $G = (V, E)$ be a graph. The **edge subdivision operation** for an edge $uv \in E$ is the deletion of uv from G and the addition of two edges uw and wv along with the new vertex w.

Note that this operation generates a new graph H:

$$H = (V \cup \{w\}, (E \backslash \{uv\}) \cup \{uw, wv\})$$

Class 1:

The following graph $G = (V, E)$, is the core graph in this class.

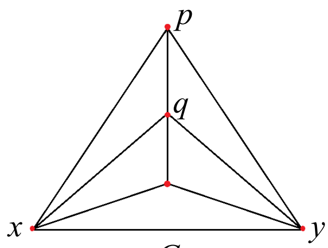

G

The members in this class can be generated by a series of edge subdivision operation for the edge pq in G and joining every new vertex to vertices x and y.

G_1 is a graph obtained by an edge subdivision operation for the edge pq in G and joining the new vertex v_1 to vertices x and y.

$$G_1 = (V \cup \{v_1\}, (E \backslash \{pq\}) \cup \{pv_1, v_1q\} \cup \{v_1x, v_1y\})$$

A graph of G_1 is provided below:

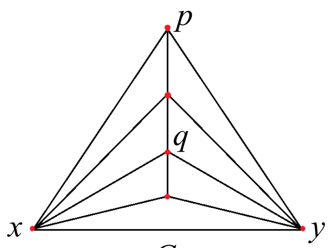

G_1

G_2 is a graph obtained by applying edge subdivision operation twice for the edge pq in G and joining every new vertex v_1 and v_2 to vertices x and y.

$$G_2 = (V \cup \{v_1, v_2\}, (E \backslash \{pq\}) \cup \{pv_1, v_1v_2, v_2q\}) \cup \{v_1x, v_1y, v_2x, v_2y\})$$

A graph of G_2 is provided:

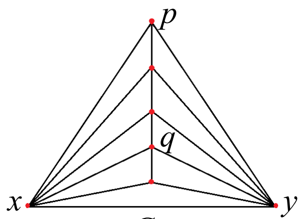

G_2

In general, for integer $\alpha \geq 1$, G_α is a graph obtained by applying edge subdivision operation α times for the edge pq in G and joining every new vertex to vertices x and y.

$$G_\alpha = (V \cup \{v_1, v_2, \ldots, v_\alpha\}, (E \backslash \{pq\}) \cup \{pv_1, v_1v_2, v_2v_3, \ldots, v_{\alpha-1}v_\alpha, v_\alpha q\} \cup \{v_1x, v_1y, v_2x, v_2y, \ldots, v_\alpha x, v_\alpha y\})$$

Note that G_α has $(\alpha + 5)$ vertices in its graph.

Proposition 1a:

A graph P is explorer if P is isomorphic to G_α, where $\alpha = 0, 2, 4, \ldots$

Class 2:
The following graph $H = (V, E)$, is the core graph in this class.

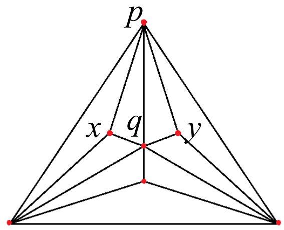

H

The members in this class can be generated by a series of edge subdivision operation for the edge pq in H and joining every new vertex to vertices x and y.

For integer $\alpha \geq 1$, H_α is a graph obtained by applying edge subdivision operation α times for the edge pq in H and joining every new vertex to vertices x and y.

$$H_\alpha = (V \cup \{v_1, v_2, \ldots, v_\alpha\}, (E \backslash \{pq\}) \cup \{pv_1, v_1v_2, v_2v_3, \ldots, v_{\alpha-1}v_\alpha, v_\alpha q\} \cup \{v_1x, v_1y, v_2x, v_2y, \ldots, v_\alpha x, v_\alpha y\})$$

A graph of H_3 is provided below:

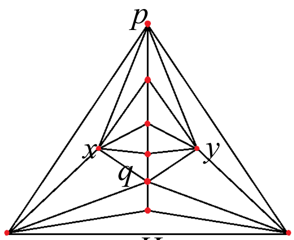

H_3

Note that H_α has $(\alpha + 7)$ vertices in its graph.

Proposition 1b:

A graph P is explorer if P is isomorphic to H_α, where $\alpha = 0, 1, 2, \ldots$

Class 3:

The following graph $K = (V, E)$, is the core graph in this class.

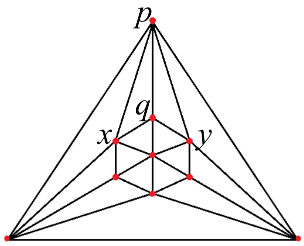

K

The members in this class can be generated by a series of edge subdivision operation for the edge pq in K and joining every new vertex to vertices x and y.

For integer $\alpha \geq 1$, K_α is a graph obtained by applying edge subdivision operation α times for the edge pq in K and joining every new vertex to vertices x and y.

$$K_\alpha = (V \cup \{v_1, v_2, \ldots, v_\alpha\}, (E \backslash \{pq\}) \cup \{pv_1, v_1v_2, v_2v_3, \ldots, v_{\alpha-1}v_\alpha, v_\alpha q\} \\ \cup \{v_1x, v_1y, v_2x, v_2y, \ldots, v_\alpha x, v_\alpha y\})$$

A graph of K_2 is provided:

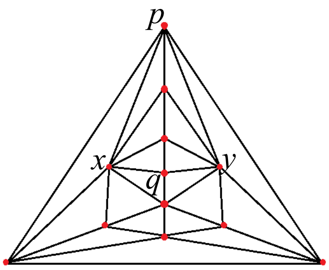

K_2

Note that K_α has $(\alpha + 10)$ vertices in its graph.

> **Proposition 1c:**
>
> A graph P is explorer if P is isomorphic to K_α, where $\alpha = 0, 2, 4, \ldots$

We present explorer graphs for class 1, 2 and 3 according to its number of vertices in the following table.

Table 1: List of Explorer Graphs against the number of vertices, v

Vertices (v)	Class 1	Class 2	Class 3
5	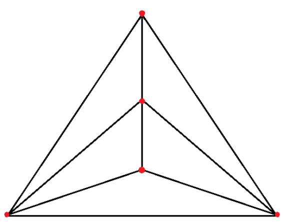		
6			

7	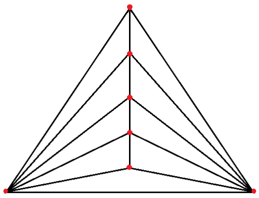	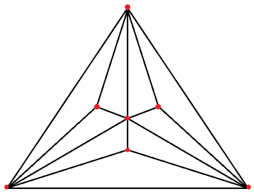	
8		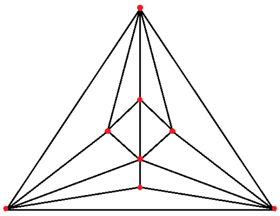	
9	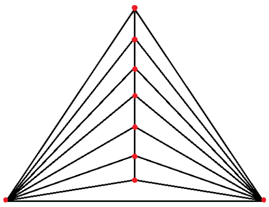	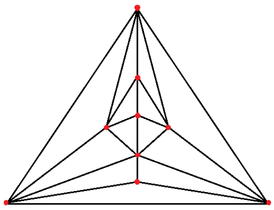	
10		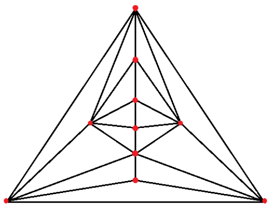	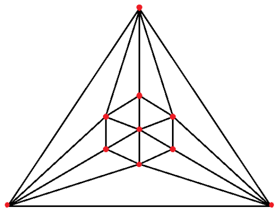
11	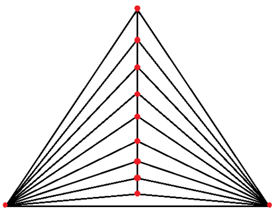	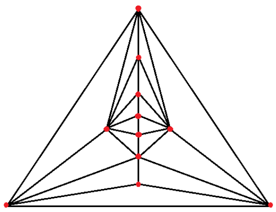	
12		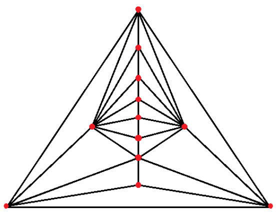	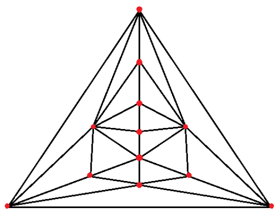
13	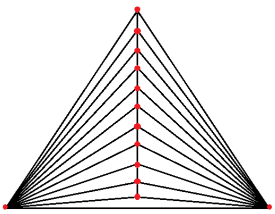	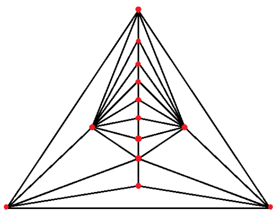	

14		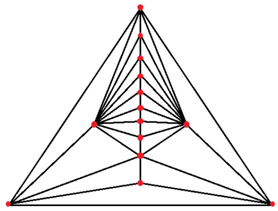	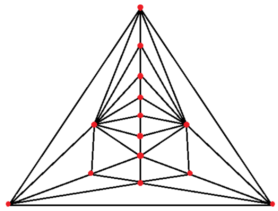
15	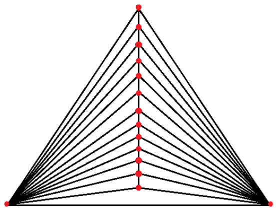	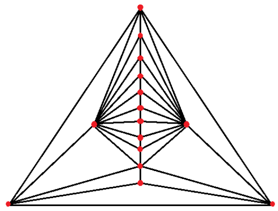	
16		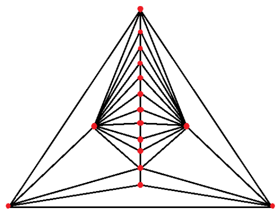	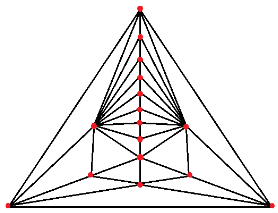

<u>2-directional classes</u>
As a corollary of *Result 2a*, we are also able to construct "2-directional classes". Class 4 is one such example.

Class 4:
The following graph $M = (V, E)$, is the core graph in this class.

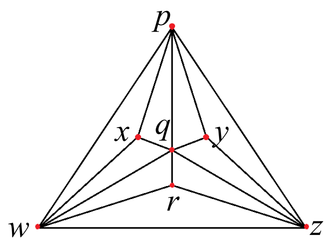

M

The members in this class can be generated by a series of edge subdivision operation for the edge pq in M and joining every new vertex to vertices x and y, followed by a series of edge subdivision operation for the edge qr in M and joining every new vertex to vertices w and z.

$M_{\alpha,0}$ is a graph obtained by applying edge subdivision operation α times for the edge pq in M and joining every new vertex to vertices x and y.

$$M_{\alpha,0} = (V \cup \{v_1, v_2, \ldots, v_\alpha\}, (E \backslash \{pq\}) \cup \{pv_1, v_1v_2, v_2v_3, \ldots, v_{\alpha-1}v_\alpha, v_\alpha q\} \cup \{v_1x, v_1y, v_2x, v_2y, \ldots, v_\alpha x, v_\alpha y\})$$

A graph of $M_{2,0}$ is provided below:

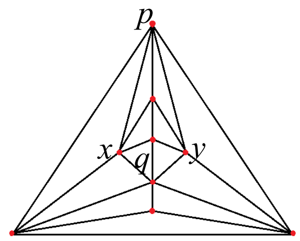

$M_{2,0}$

$M_{0,\beta}$ is a graph obtained by applying edge subdivision operation β times for the edge qr in M and joining every new vertex to vertices w and z.

$$M_{0,\beta} = (V \cup \{v_1, v_2, \ldots, v_\beta\}, (E \backslash \{qr\}) \cup \{qv_1, v_1v_2, v_2v_3, \ldots, v_{\beta\text{-}1}v_\beta, v_\beta r\} \cup \{v_1w, v_1z, v_2w, v_2z, \ldots, v_\beta w, v_\beta z\})$$

A graph of $M_{0,2}$ is provided below:

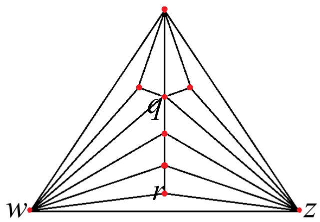

$M_{0,2}$

For integer $\alpha \geq 1$ and $\beta \geq 1$, $M_{\alpha,\beta}$ is a graph obtained by first applying edge subdivision operation α times for the edge pq in M and joining every new vertex to vertices x and y, then applying edge subdivision operation β times for the edge qr in the resultant graph and joining every new vertex to vertices w and z.

$$M_{\alpha,\beta} = (V \cup \{v_1, v_2, \ldots, v_\alpha\} \cup \{v_{\alpha+1}, v_{\alpha+2}, \ldots, v_{\alpha+\beta}\}, (E \backslash \{pq, qr\}) \cup \{pv_1, v_1v_2, v_2v_3, \ldots, v_{\alpha\text{-}1}v_\alpha, v_\alpha q\} \cup \{v_1x, v_1y, v_2x, v_2y, \ldots, v_\alpha x, v_\alpha y\} \cup \{qv_{\alpha+1}, v_{\alpha+1}v_{\alpha+2}, v_{\alpha+2}v_{\alpha+3}, \ldots, v_{\alpha+\beta\text{-}1}v_{\alpha+\beta}, v_{\alpha+\beta}r\} \cup \{v_{\alpha+1}w, v_{\alpha+1}z, v_{\alpha+2}w, v_{\alpha+2}z, \ldots, v_{\alpha+\beta}w, v_{\alpha+\beta}z\})$$

A graph of $M_{2,2}$ is provided below:

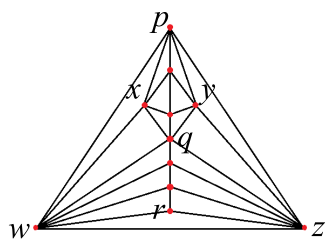

$M_{2,2}$

Note that $M_{\alpha,\beta}$ has $(\alpha + \beta + 7)$ vertices in its graph.

Proposition 2:

A graph P is explorer if P is isomorphic to $M_{\alpha,\beta}$, where

$$\begin{cases} \beta = 0, 2, 4, 6, \ldots, if\ \alpha = 0, 2, 4, 6, \ldots \\ \beta = 0, 1, 2, 3, \ldots, if\ \alpha = 1, 3, 5, 7, \ldots \end{cases}$$

We present explorer graphs for class 4 according to its number of vertices in the *Table 2*. As compared to classes 1, 2 and 3, class 4 generates more non-isomorphic explorer graphs for a high enough number of vertices. It is easily observable that there are infinitely many explorer graphs. In fact, they make up a significant portion of maximal planar graphs. There exist, for example, at least 6 non-isomorphic explorer graphs for 11 vertices just from *Table 1* and *Table 2*.

Table 2: List of Class 4 of Explorer Graphs against the number of vertices, v

Vertices (v)	$\alpha = 0$	$\alpha = 1$	$\alpha = 2$	$\alpha = 3$
7	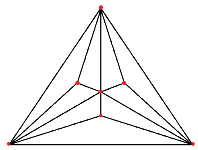 $\beta = 0$			
8		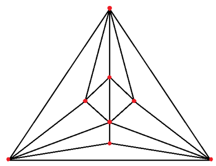 $\beta = 0$		
9	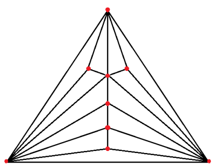 $\beta = 2$	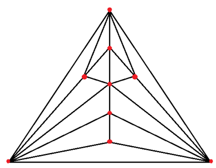 $\beta = 1$	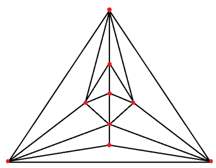 $\beta = 0$	
10		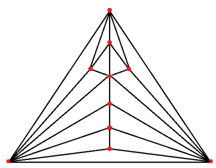 $\beta = 2$		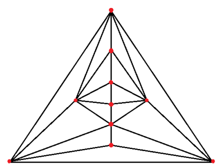 $\beta = 0$
11	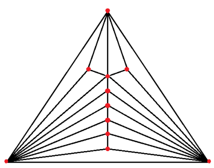 $\beta = 4$	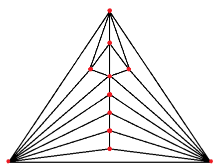 $\beta = 3$	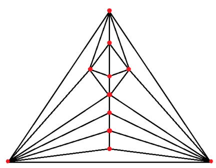 $\beta = 2$	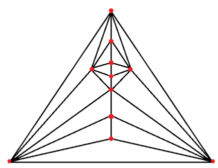 $\beta = 1$
12		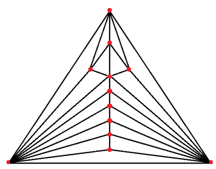 $\beta = 4$		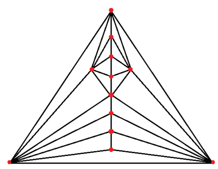 $\beta = 2$
13	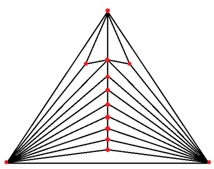 $\beta = 6$	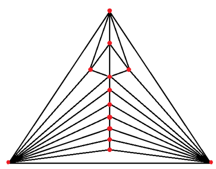 $\beta = 5$	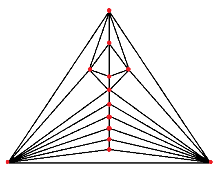 $\beta = 4$	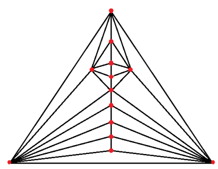 $\beta = 3$

Line Graph of a Maximal Planar Graph

The rules of an explorer walk are so far directed and restrictive, but not well represented. The major consideration of tracing an explorer walk in a maximal planar graph is the adjacency of edges, and less of the orientation of vertices. This serves as a motivation for us to explore the problem in the context of line graphs. The definition of a **line graph** is as follows:

"Each edge in a maximal planar graph is represented by a vertex in the line graph. Two vertices in the line graph are adjacent if and only if the corresponding two edges in the maximal planar graph are incident."

Let L(P) be a line graph of a maximal planar graph, P. An explorer walk in the maximal planar graph corresponds to a close walk in L(P). A restricted line graph of P, **$L_R(P)$**, can be constructed under the following definition:

> **Definition 3:**
>
> L(P) and $L_R(P)$ shares the same set of vertices. Two vertices in $L_R(P)$ are adjacent if and only if the corresponding two edges in the maximal planar graph are edges of a common face.

Figure 9 shows an example of an explorer graph G with vertices P_1, P_2, P_3, …, P_9, and the corresponding $L_R(G)$. The vertices of $L_R(G)$ are labelled as "P_mP_n", $m, n \in \mathbb{Z}^+$, $1 \le m < n \le 9$, where P_mP_n is an edge in G that connects P_m and P_n.

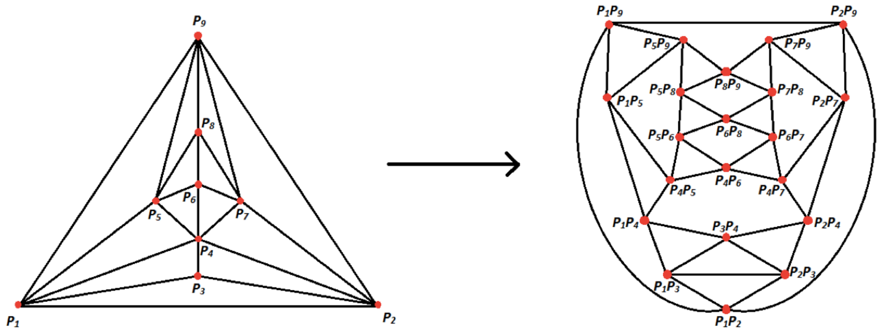

G **$L_R(G)$**

Figure 9

Here, we have some necessary conditions for $L_R(P)$:

> **Proposition 3:**
>
> Given any maximal planar graph P, $L_R(P)$ must satisfy the following:
> 1. It is a 4-regular planar graph
> 2. Any edge is an edge of at least one C_3
> 3. The explorer walk in P corresponds to a restricted walk in $L_R(P)$, pre-determined by the first move (you don't have to refer to P for directions while tracing the walk in $L_R(P)$)

Moreover, $L_R(P)$ is an Eulerian graph (as it is 4-regular). With that, we have the following result (For proof, refer to "Appendix"):

> **Result 3:**
>
> An explorer walk in P (of order $n \ge 4$) corresponds to an Eulerian circuit in $L_R(P)$ if and only if P is an explorer graph.

With that, we are now able to more properly restate our problem statement as the following:

> **Revised Problem Statement 2:**
>
> Our research aims to find maximal planar graphs, P, such that the explorer walk in P corresponds to an Eulerian circuit in $L_R(P)$.

<u>Edge Contraction of Explorer Graphs</u>

The paper has, thus far, been analyzing explorer graphs due to their volumetric properties. Nonetheless, we are still able to calculate the volume of triangulated polyhedrons, whose skeletons are non-explorer graphs, via explorer graphs of higher order. This is made possible through edge contraction.

It is important to note that applying an edge contraction on a maximal planar graph does not necessary produce another maximal planar graph. The resultant graph is, nonetheless, still a planar graph due to Kuratowski's Theorem [9].

> **Result 4:**
>
> Given any vertex, v, in a maximal planar graph P of order $n \geq 4$, there exists <u>at least</u> one edge, incident with v, whose contraction produces another maximal planar graph.

The above result has important consequences. For a maximal planar graph, of order $n \geq 5$, there always exist a way to obtain the graph of a triangular bipyramid (which is of order 5) through $n - 5$ edge contractions, without losing the identity of maximal planar graph in the process. *Conjecture 1*, which is to be presented, is built on this fact.

> **Definition 4:**
>
> A ***k*-Induced Maximal Planar Graph** is a maximal planar graph, of order $n \geq 4$, whose construction requires <u>at least</u> $k \in \mathbb{Z}$, $k \geq 0$, edge contraction operations from any explorer graph.

By convention, we define a maximal planar graph to be explorer when $k = 0$. A maximal planar graph is non-explorer when $k \geq 1$.

Figure 10 below illustrates a 1-induced maximal planar graph (on the right) obtained from only 1 contraction of edge QR of an explorer graph (on the left).

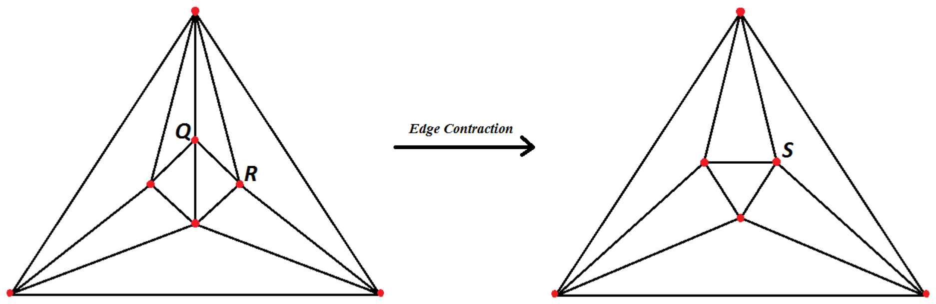

Figure 10

After verifications of non-explorer graphs with small number of vertices, we have the following result:

Proposition 4:

A maximal planar graph, P, with $4 \leq n \leq 8$ vertices, $n \in \mathbb{Z}^+$, is either explorer or 1-induced.

Not all non-explorer graphs are 1-induced. Icosahedron graph, for example, is a 2-induced maximal planar graph. To seek a more generalized form of *Proposition 4*, we have the following conjecture (For the incomplete proof, refer to "Appendix"):

Conjecture 1:

A maximal planar graph, P, of order $n \geq 5$, is k-induced, where $k \leq 3n - 15$, $k \in \mathbb{Z}^+$.

<u>Explorer Graph to Polyhedrons</u>

Recall that Steiniz's Theorem states that "every 3-connected planar graph can be represented as the graph of a convex polyhedron", and explorer graphs are 3-connected. We have also mentioned that it is possible to have two topologically distinct polyhedrons that corresponds to the same maximal planar graph after triangulation. For instance, a quadrilateral-based pyramid, after triangulation, shares the same maximal planar graph as a triangular bipyramid.

In this section, we provide examples of polyhedrons constructed from explorer graphs and verify that the explorer walk in these graphs give rise to the volume of the constructed polyhedrons. In contrast, we will also provide examples of polyhedrons constructed from non-explorer graphs and verify that the explorer walk in these graphs might not give rise to the volume of the constructed polyhedrons.

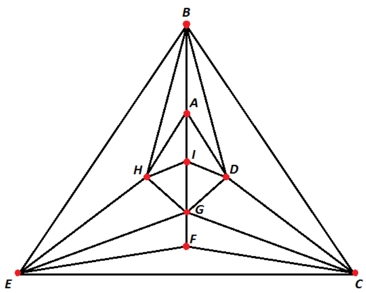

Figure 11

Figure 11 shows an explorer graph that can be constructed into an elongated pyramid (Figure 12) with vertices of coordinates *A(–2, 5, 2)*, *B(–5, –1, –5)*, *C(3, 1, –10)*, *D(6, 7, –3)*, *E(–2, –8, –3)*, *F(6, –6, –8)*, *G(9, 0, –1)*, *H(1, –2, 4)* and *I(8, 9, 7)*. The volume is calculated to be $961 cm^3$ using *GeoGebra*. The following sequence can be obtained through an explorer walk in the graph:

"*ECFGEHBADIGHEBCDGIHABD*
CGFECBDAIHGEFCGDIAHBEC"

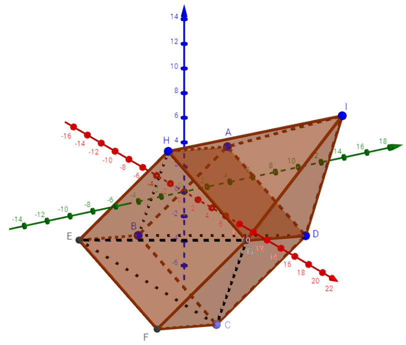

Figure 12

Hence, the volume can also be calculated as such:

$$Volume = \frac{1}{6}\,|\,ECFGEHBADIGHEBCDGIHABD$$

$$CGFECBDAIHGEFCGDIAHBEC\,|$$

$$= \frac{1}{6}\left[(3694)-(-2072)\right] \quad 961\ cm^3$$

3694 is the sum of down products while –2072 is the sum of up products in the matrix.

Similarly, the formula can be applied to any other elongated quadrilateral pyramid and triangulated polyhedrons sharing an isomorphic maximal planar graph as their skeletons.

Figure 13 shows a non-explorer graph that can be constructed into a prism (*Figure 14*) with vertices of coordinates *A(–3, 1, 3)*, *B(3, –9, 1)*, *C(3, 0, –2)*, *D(8, –4, 4)*, *E(8, 5, 1)* and *F(2, 6,* 6). The volume is calculated to be 246cm^3 using *GeoGebra*. The following sequence can be obtained through an explorer walk in the graph:

"*FEACBDFE*"

However, the value calculated from the matrix is:

$$\frac{1}{6}\left|FEACBDFE\right| = \frac{1}{6}\left[(297)-(-174)\right] \quad 78\frac{1}{2}\ cm^3$$

297 is the sum of down products while –174 is the sum of up products in the matrix.

It is known that there exists no explorer graph with 6 vertices. Nonetheless, explorer graphs with higher number of vertices can still be used to calculate the prism's volume. This is a result of the property of edge contraction.

For example, the non-explorer graph shown in Figure 13 is a result of 3 edge contractions from the explorer graph shown in Figure 15, which is a relabeled graph of the elongated pyramid. (Edges *AA'*, *CC'* and *CC''* are contracted).

In the calculations, we are still making use of the matrix formed from the explorer walk in the explorer graph, but we now unify the coordinates of the vertices with those of the vertices that they are merged with (e.g. *A'* shares the same coordinates as *A*):

$$Volume = \frac{1}{6}\,|\,FEA'AFBDC''CC'ABFDECAC'BC''DC$$

$$EAA'FEDCC''C'BAFA'EACC'C''BDFE\,|$$

$$= \frac{1}{6}\left[(790)-(-686)\right] \quad 246cm^3$$

790 is the sum of down products while –686 is the sum of up products in the matrix.

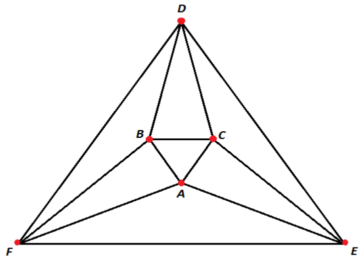

Figure 13

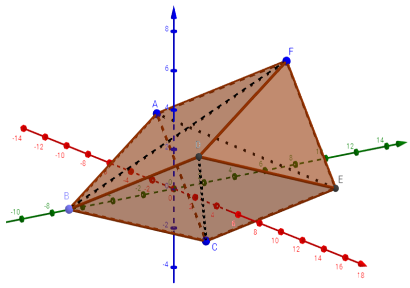

Figure 14

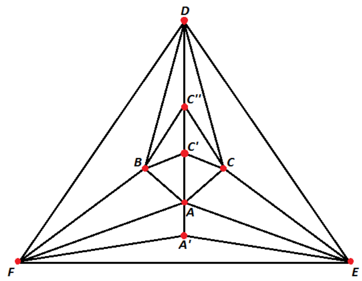

Figure 15

This technique allows us to cover a significantly wider range of polyhedrons (although we can't confirm the conjecture that it covers all convex polyhedrons) whose volume can be solved via the means of explorer graphs.

Conclusion

In this paper, we developed an explorer walk in a maximal planar graph. As a result, we uncovered a family of graphs, which are the explorer graphs, that contains volumetric properties in regard to the explorer walk. The volumetric aspect is, however, treated as a by-product made possible through the *Alternating Shoelace Method*. The explorer walk corresponding to an Eulerian circuit in the restricted line graph is what truly defines explorer graphs. Despite the explorer walk being restrictive, the explorer graphs make up a significant portion of the maximal planar graphs. To illustrate that, we proposed different constructions of explorer graphs from that of a lower order. For future research, the topology of explorer graphs can be studied in greater details. For that, we wish to prove or disprove *Conjecture 1*, or find a better bound for the value of k for k-induced maximal planar graph of order n.

References

[1] Chazelle, Bernard. "Triangulating a simple polygon in linear time." *Discrete & Computational Geometry* 6.3 (1991): 485-524.

[2] Grünbaum, Branko, et al. *Convex polytopes*. Vol. 16. New York: Interscience (1967)

[3] Richeson, David S. "Euler's gem." *The polyhedron formula* (2008).

[4] De Loera, Jesús A., Jörg Rambau, and Francisco Santos Leal. "Triangulations." (2004).

[5] Sloane, N. J. A. Sequence A000109/M1469 in "The On-Line Encyclopedia of Integer Sequences." Accessed 31 Aug. 17.

[6] Stojanović, Milica. "Algorithms for triangulating polyhedra into a small number of tetrahedra." *Matematički vesnik* 57.1-2 (2005): 1-9.

[7] Keil, J. Mark, and Timothy B. Brecht. "The complexity of clustering in planar graphs." *J. Combinatorial Mathematics and Combinatorial Computing* 9 (1991): 155-159.

[8] Rosen, Kenneth H. "Discrete mathematics and its applications." *AMC* 10 (2007): 12.

[9] Thomassen, Carsten. "Kuratowski's theorem." *Journal of Graph Theory* 5.3 (1981): 225-241.

Appendix

Proof of "Result 1"

We shall first prove that if the explorer order generates $3F + 2$ points (mentions $3F$ triangular faces in the matrix) for a polyhedron with F faces after triangulation, it will mention each triangular face exactly thrice in the matrix.

i) An explorer order is unique based on the first three chosen points in the matrix, as each subsequent point is determined by the three points before it. (Every edge is shared by exactly 2 surface triangles)

ii) If a surface triangle $P_1P_2P_3$ is mentioned in order of "$P_1P_2P_3$" in the matrix, it will not be mentioned in the reverse order of "$P_3P_2P_1$" in the same matrix. Suppose the reverse order exists in the same matrix. Without loss of generality, suppose "$P_1P_2P_3$" appears before "$P_3P_2P_1$".

$$|\ldots P_1P_2P_3\ldots P_3P_2P_1\ldots|$$

The subsequent points generated after "$P_1P_2P_3$" and before "$P_3P_2P_1$" are determined and symmetric, and hence does not converge to form consecutive 3 distinct points (representing a surface triangle) that is non-symmetric. This contradicts with the condition that any consecutive three points in the matrix corresponds to a surface triangle.

iii) No three consecutive points is mentioned twice in the matrix in the same order. It's obvious that the first three chosen points will not be mentioned twice in the same order by the rules of an explorer order. Now, suppose "$P_iP_jP_k$" is mentioned twice in the matrix.

$$|\ldots P_iP_jP_k \ldots P_iP_jP_k \ldots|$$

The subsequent points generated before "$P_iP_jP_k$" and "$P_iP_jP_k$" are determined and unique, which means the first three points are also mentioned twice in the same order. This is a contradiction.

iv) A surface triangle $P_1P_2P_3$ can only be mentioned in three distinct ways (the reverse order is considered as equivalent) – "$P_1P_2P_3$", "$P_2P_3P_1$" or "$P_3P_1P_2$". If a surface triangle is mentioned less than thrice, there exist some other surface triangle that is mentioned more than thrice, and hence in more than three distinct ways. This is a contradiction.

Now we have concluded that each triangular face is mentioned exactly thrice in three distinct ways if the explorer order generates $3F + 2$ points for a polyhedron with F faces after triangulation.

For the second part of our proof, we recall the set of notations for the **polarity** of the cross multiplication in our matrix. For any 3 points (may not be distinct) P_1, P_2 and P_3:

$$|P_1P_2P_3|^+ = \begin{vmatrix} x_1 & x_2 & x_3 \\ y_1 & y_2 & y_3 \\ z_1 & z_2 & z_3 \end{vmatrix} = \left(x_1y_2z_3 \quad x_3y_2z_1\right) \text{ and } |P_1P_2P_3|^- = \begin{vmatrix} x_1 & x_2 & x_3 \\ y_1 & y_2 & y_3 \\ z_1 & z_2 & z_3 \end{vmatrix} = \left(x_3y_2z_1 \quad x_1y_2z_3\right)$$

The above matrixes can be interpreted as products represented by diagonal arrows pointing downwards subtracting products represented by diagonal arrows pointing upwards.

It's clear that

$$|P_1P_2P_3|^+ = |P_3P_2P_1|^-$$

Referring to *Figure A1*, we have two adjacent triangular faces $P_1P_2P_3$ and $P_2P_3P_4$ where P_1, P_2, P_3 and P_4 are distinct. According to the explorer order, if the first three points in the matrix is not "$P_2P_3P_4$", and "$P_1P_2P_3$" is mentioned in the matrix, the next mentioned point must be P_4. If "$P_1P_2P_3$" is anti-clockwise on the surface triangle $P_1P_2P_3$, then "$P_2P_3P_4$" must be clockwise on the surface triangle $P_2P_3P_4$, and vice versa.

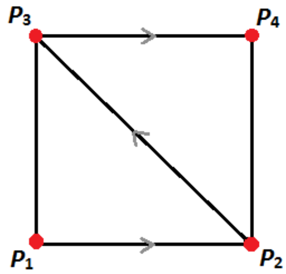

Figure A1

According to the explorer order, the first three points in the matrix corresponds to a triangular face in the anti-clockwise manner. Suppose our matrix generated by explorer order is as follows:

$$|P_1P_2P_3...P_n| = |P_1P_2P_3|^+ + |P_2P_3P_4|^- + |P_3P_4P_5|^+ + |P_4P_5P_6|^- + ... + |P_{n-2}\overset{\pm}{}P_{n-1}P_n|$$

We have $|P_1P_2P_3|^+$ in the positive polarity. It is now obvious that any consecutive three points in the matrix that corresponds to a triangular face in the anti-clockwise manner is positive in polarity, and any consecutive three points that corresponds to a triangular face in the clockwise manner is negative in polarity.

Now we have

$$\det|P_1P_2P_3| = |P_1P_2P_3|^+ + |P_2P_3P_1|^+ + |P_3P_1P_2|^+$$

Since each triangular face (triangle $P_1P_2P_3$ for example) is mentioned exactly thrice in three distinct ways if the explorer order generates $3F + 2$ points for a polyhedron with F faces after triangulation, the matrix must also contain $|P_1P_2P_3|^+ = |P_3P_2P_1|^-$, $|P_2P_3P_1|^+ = |P_1P_3P_2|^-$ and $|P_3P_1P_2|^+ = |P_2P_1P_3|^-$. Hence, the determinants applied on all triangular surfaces in the anti-clockwise manner will be mentioned in the matrix.

Hence, by multiplying *1/6* to the matrix, we can conclude that an explorer order gives volume to a triangulated polyhedron if it generates $3F + 2$ points.

<u>Proof of "Result 2a and 2b"</u>

For Result 2a, the string of edge contraction includes the addition of 4 new vertices B_1, B_2, B_3 and B_4. (Figure A2) It suffices to prove that the explorer walk on the new graph generates 24 more points, according to Definition 2 in the report.

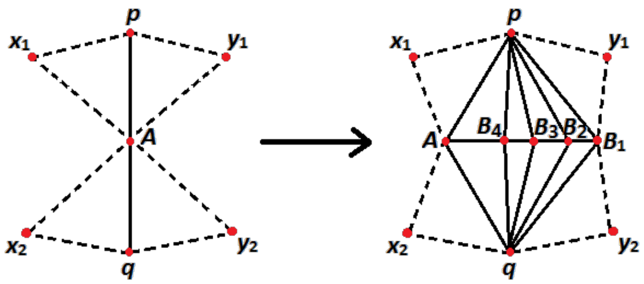

Figure A2

In the explorer walk before the "inverse" edge contraction, "x_2Aq" must be mentioned either in that or in the reverse order, but are treated as equivalent without loss of generality. In certain cases, the set $X = \{x_1, x_2, x_3, \ldots, x_m\}$ may be empty, in which we can treat x_2 as p. After the "inverse" edge contraction, "x_2Aq" is replaced by "$x_2AqB_4B_3pB_2B_1q$" without affecting the subsequent points that come after and before. At the same time, 6 additional points are introduced. Similarly, "x_2qA" is replaced by "$x_2qAB_4pB_3B_2qB_1$" without affecting the subsequent points that come after and before, with 6 additional points being introduced at the same time. "x_1pA" is replaced by "$x_1pAB_4qB_3B_2pB_1$" without affecting the subsequent points that come after and before, with 6 additional points being introduced at the same time. "x_1Ap" is replaced by "$x_1ApB_4B_3qB_2B_1p$" without affecting the subsequent points that come after and before, with 6 additional points being introduced at the same time. In total, 24 new points are introduced. The conclusion follows.

Similarly, for Result 2b, the string of edge contraction includes the addition of 4 new vertices B_1, B_2, B_3 and B_4. (Figure A3) It suffices to prove that the explorer walk on the new graph generates 24 more points, according to Definition 2 in the report.

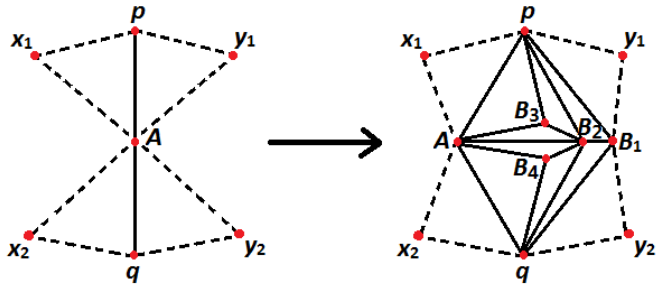

Figure A3

In the explorer walk before the "inverse" edge contraction, "x_2Aq" must be mentioned either in that or in the reverse order, but are treated as equivalent without loss of generality. In certain cases, the set $X = \{x_1, x_2, x_3, \ldots, x_m\}$ may be empty, in which we can treat x_2 as p. After the "inverse" edge contraction, "x_2Aq" is replaced by "$x_2AqB_4B_2AB_3pB_2B_1q$" without affecting the subsequent points that come after and before. At the same time, 8 additional points are introduced. Similarly, "x_2qA" is replaced by "$x_2qAB_4B_2qB_1$" without affecting the subsequent points that come after and before, with 4 additional points being introduced at the same time. "x_1pA" is replaced by "$x_1pAB_3B_2pB_1$" without affecting the subsequent points that come after and before, with 4 additional points being introduced at the same time. "x_1Ap" is replaced by "$x_1ApB_3B_2AB_4qB_2B_1p$" without affecting the subsequent points that come after and before, with 8 additional points being introduced at the same time. In total, 24 new points are introduced. The conclusion follows.

<u>Proof of "Result 3"</u>

The proof revolves around the equivalence of tracing an explorer walk in a maximal planar graph, P, and its specialized line graph, $L_R(P)$. From the proof of *Result 1* we know that for an explorer walk in a triangulated graph:

i) No three consecutive points is mentioned twice in the matrix in the same order
ii) If a surface triangle $P_1P_2P_3$ is mentioned in order of "$P_1P_2P_3$" in the matrix, it will not be mentioned in the reverse order of "$P_3P_2P_1$" in the same matrix

We can therefore conclude that in $L_R(P)$, **no edge will be travelled twice** in an explorer walk. Also, it is known that P must contain $3f/2$ edges since P is a maximal planar graph, where f is the number of faces of P. Hence, $L_R(P)$ must contain $3f/2$ vertices. Since $L_R(P)$ is 4-regular, it contains **$3f$ edges** by handshaking lemma.

We can now conclude that P is an explorer graph <u>if and only if</u> an explorer walk in P will generate $3f - 2$ points, and therefore mention $3f - 1$ edges of P ($3f - 1$ vertices of $L_R(P)$) in the matrix. That's is also equivalent to travelling $3f$ edges in $L_R(P)$, creating an Eulerian circuit.

<u>Proof of "Result 4"</u>

For a maximal planar graph to remain as a maximal planar graph after an edge contraction, the number of edges must decrease by 3 together with the loss of 1 vertex in the edge contraction.

We claim that given any vertex, v, in a maximal planar graph P of order $n \geq 4$, there exists at least one edge, incident with v, whose contraction produces another maximal planar graph.

If $d(v) = 3$,

Any edge incident with v can be contracted, since the edge contraction is the loss of v and the 3 edges incident to it.

If $d(v) = 4$,

Suppose that v is adjacent to the set of vertices $\{v_1, v_2, v_3, v_4\}$. (Figure A4) Say that vv_1 is the edge we choose to contract. Since we only desire a loss of 3 edges, it is easy to see that vv_1 can be contracted if and only if v_1 is not adjacent to v_4. Suppose none of the edges vv_1, vv_2, vv_3 or vv_4 can be contracted, v_1, v_2, v_3 and v_4 must be adjacent to each other, forming a K_5 with v. By Kuratowski's Theorem, P is non-planar. Contradiction!

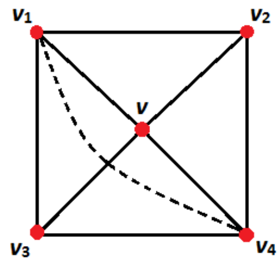

Figure A4

If $d(v) \geq 5$,

Suppose that v is adjacent to the set of vertices $\{v_1, v_2, v_3, \ldots, v_n\}$, for $n \geq 5$ (Figure A5). We aim to prove that if none of the edges vv_1, vv_2, vv_3, …, vv_n can be contracted, P must contain $K_{3,3}$ as a minor.

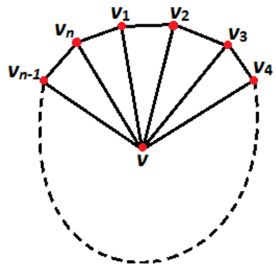

Figure A5

vv_1 can be contracted if and only if v_1 is adjacent to only v_2 and v_n in the set $\{v_1, v_2, v_3, \ldots, v_n\}$. vv_n can be contracted if and only if v_n is adjacent to only v_1 and v_{n-1} in the set $\{v_1, v_2, v_3, \ldots, v_n\}$. For $2 \leq i \leq n-1$, vv_i can be contracted if and only if v_i is adjacent to only v_{i-1} and v_{i+1} in the set $\{v_1, v_2, v_3, \ldots, v_n\}$.

If none of the edges vv_1, vv_2, vv_3, …, vv_n can be contracted, there must exist two edges v_jv_k and v_pv_q for some $1 \leq j < p < k < q \leq n$, forming a crossing. Suppose no such 2 edges exist, let v_1 be connected to v_i for some $3 \leq i \leq n-1$ (Figure A6). v_2 must be connected to v_j for some $4 \leq j \leq i$. v_3 must then be connected to v_k for some $5 \leq k \leq j$. v_4 must then be connected to v_p for some $6 \leq p \leq k$. So on… In the end, there must exist a q such that v_q can only be connected to v_{q+2}. v_{q+1} can only be connected to v_q and v_{q+2} in the vertices set $\{v_1, v_2, v_3, \ldots, v_n\}$. Contradiction!

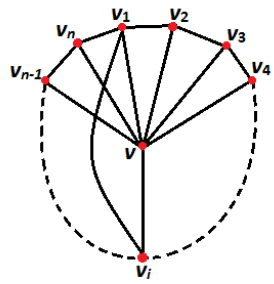

Figure A6

Now that there must exist two edges v_jv_k and v_pv_q for some $1 \leq j < p < k < q \leq n$, which forms a crossing, there must also exists a v_r that is distinct from $\{v_j, v_p, v_k, v_q\}$ since $d(v) \geq 5$. WLOG, assume $p < r < k$. Now we contract the set of edges $\{v_1v_2, v_2v_3, v_3v_4, \ldots, v_{p-2}v_{p-1}\}$ into v_j, $\{v_pv_{p+1}, v_{p+1}v_{p+2}, v_{p+2}v_{p+3}, \ldots, v_{r-2}v_{r-1}\}$ into v_p, $\{v_rv_{r+1}, v_{r+1}v_{r+2}, v_{r+2}v_{r+3}, \ldots, v_{k-2}v_{k-1}\}$ into v_r, $\{v_kv_{k+1}, v_{k+1}v_{k+2}, v_{k+2}v_{k+3}, \ldots, v_{q-2}v_{q-1}\}$ into v_k, and $\{v_qv_{q+1}, v_{q+1}v_{q+2}, v_{q+2}v_{q+3}, \ldots, v_{n-1}v_n\}$ into v_q. Finally, a $K_{3,3}$ can be formed by taking $X = \{v_j, v_q, v_r\}$ and $Y = \{v_p, v_k, v\}$ (Figure A7). Since P contains $K_{3,3}$ as a minor, P is non-planar by Kuratowski's Theorem. Contradiction!

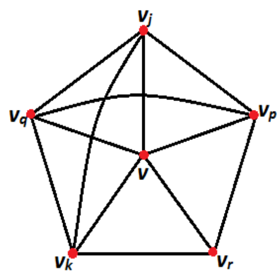

Figure A7

The conclusion follows.

Incomplete proof of "Conjecture 1"

Suppose G is a non-explorer graph with $n \geq 5$ vertices. The graph of triangular bipyramid (Figure A8), also known as the J_{12} (Johnson solid) skeleton, can be obtained via edge contraction of G without losing the identity of maximal planar graph in the process. (*Result 4*) Now we want to construct G from J_{12} skeleton via the *"inverse" edge contractions*.

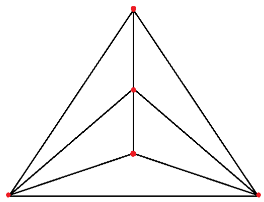

Figure A8

Building Vertices Groups: (*Result 2a*)

For any explorer graph, P, applying the following string of "inverse" edge contraction on any vertex results in another explorer graph. (Figure A9)

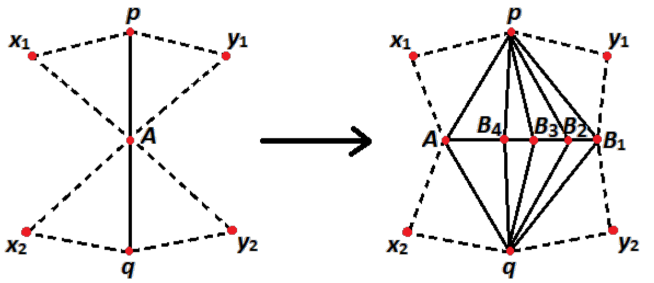

Figure A9

The newly created 4 vertices can be treated as "vertices group B". We can notate "vertices group B" as follows:

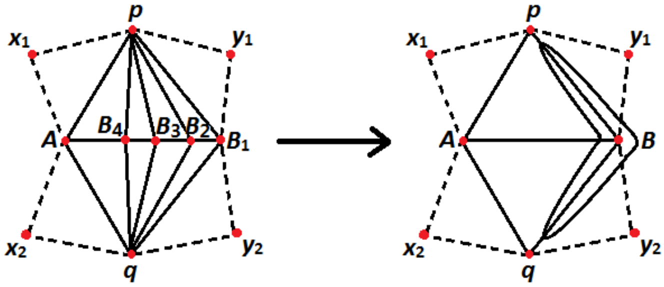

Figure A10

We construct G via the "inverse" edge contractions, in an order opposite of a certain edge contraction of G to J_{12} skeleton. However, by creating <u>vertices groups</u> instead of vertices, we hope to generate an explorer graph, G', of order $4n - 15$. If successful, G can then be obtained via edge contractions of <u>all vertices groups</u> into vertices in G'.

A vertices group consists of 4 vertices and 2 "wings". In Figure A10, for example, edges Bp and Bq are the wings of vertices group B (which contains 4 vertices). Figure A11 is a further illustration on "vertices groups":

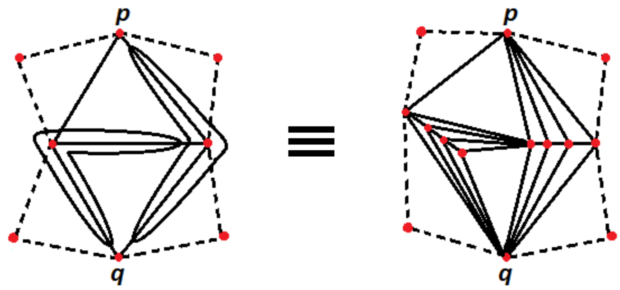

Figure A11

Now, it suffices to prove that it's always possible to generate a "vertices group" instead of a vertex in an "inverse" edge contraction.

Referring to Figure A9, say that the vertex *A* and the edges *Ap* and *Aq* are involved in the "inverse" edge contraction. If *A* is not a vertices group, "inverse" edge contraction can be performed as demonstrated in Figure A9. Now suppose *A* is a vertices group.

Case 1:

If *Ap* and *Aq* are wings of the vertices group *A*, the "inverse" edge contraction can be performed as follows:

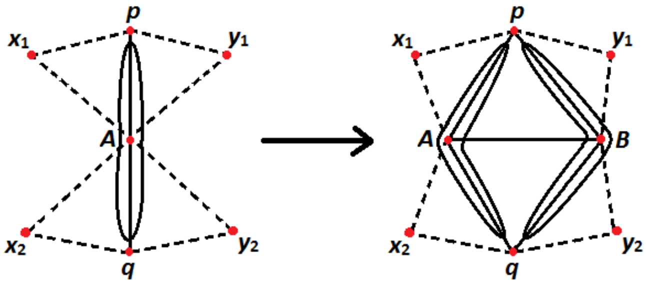

Figure A12

Case 2:

If only one of the edges, *Ap* or *Aq*, (say *Ap*) is a wing of the vertices group *A*, the other wing can either be on the side of *X* or *Y* (say *X*). (Figure A13) The "inverse" edge contraction can be performed in the direction of *Y*, opposite to the wing.

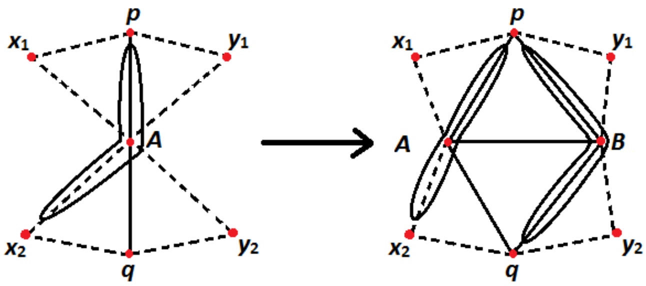

Figure A13

Case 3:

If none of the edges, *Ap* or *Aq*, is a wing of the vertices group *A*, the wings can either be both on the same side (*X* or *Y*), or one on each side. If the wings of *A* are both on the same side (say *X*), the "inverse" edge contraction can be performed in the direction of *Y*, opposite to the wings. (Figure A14)

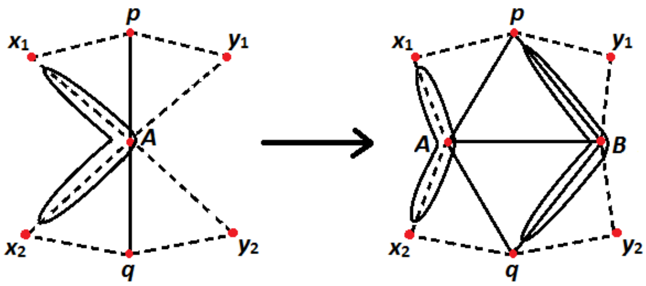

Figure A14

Case 4 (Unsolved Case):

We have yet to find a way to perform the "inverse" edge contraction if the wings of the vertices group *A* lies on both *X* and *Y*. If there's a way, Conjecture 1 can then be completely proven.

Acknowledgement
I would like to thank my mentor, Mr. Chia Vui Leong, for his supervision throughout the research, and NUS High School for providing me the opportunity and constant support that made this project possible.